



Modeling impacts of climate change on freshwater availability in Africa

Monireh Faramarzi^{a,*}, Karim C. Abbaspour^b, Saeid Ashraf Vaghefi^{b,c}, Mohammad Reza Farzaneh^a, Alexander J.B. Zehnder^{d,e}, Raghavan Srinivasan^f, Hong Yang^{b,g}

^a Department of Natural Resources, Isfahan University of Technology, 84156 Isfahan, Iran

^b Eawag, Swiss Federal Institute of Aquatic Science and Technology, P.O. Box 611, 8600 Dübendorf, Switzerland

^c Department of Civil & Environmental Engineering, Amirkabir University of Technology, Tehran, Iran

^d Alberta Water Research Institute (AWRI), Edmonton, AB T5N 1M9, Canada

^e Nanyang Technological University (NTU), Sustainable Earth Office, Singapore 637459, Singapore

^f Spatial Science Laboratory, Texas A&M University, College Station, TX, USA

^g Faculty of Science, University of Basel, Switzerland

ARTICLE INFO

Article history:

Received 12 February 2012

Received in revised form 21 November 2012

Accepted 8 December 2012

Available online 19 December 2012

This manuscript was handled by Konstantine P. Georgakakos, Editor-in-Chief, with the assistance of David J. Gochis, Associate Editor

Keywords:

Water balance

SWAT

Water resources

SUMMARY

This study analyzes the impact of climate change on freshwater availability in Africa at the subbasin level for the period of 2020–2040. Future climate projections from five global circulation models (GCMs) under the four IPCC emission scenarios were fed into an existing SWAT hydrological model to project the impact on different components of water resources across the African continent. The GCMs have been down-scaled based on observed data of Climate Research Unit to represent local climate conditions at 0.5° grid spatial resolution. The results show that for Africa as a whole, the mean total quantity of water resources is likely to increase. For individual subbasins and countries, variations are substantial. Although uncertainties are high in the simulated results, we found that in many regions/countries, most of the climate scenarios projected the same direction of changes in water resources, suggesting a relatively high confidence in the projections. The assessment of the number of dry days and the frequency of their occurrences suggests an increase in the drought events and their duration in the future. Overall, the dry regions have higher uncertainties than the wet regions in the projected impacts on water resources. This poses additional challenge to the agriculture in dry regions where water shortage is already severe while irrigation is expected to become more important to stabilize and increase food production.

© 2012 Elsevier B.V. All rights reserved.

1. Introduction

Africa is home to 600 million people experiencing water scarcity (World Bank, 1995; IPCC, 2007), and in the Sub-Saharan Africa alone over 260 million people are undernourished (FAO, 2006). Unreliable rainfall patterns, uneven distribution of water resources, weather variability, and human factors such as population growth and tensions over the shared waters present a significant concern for the availability, access, and utilization of water resources. This has a direct impact on the livelihoods of many, particularly the poor people in Africa (Vörösmarty et al., 2005, 2010; Milly et al., 2005; Boko et al., 2007; Ziervogel et al., 2010). Climate change and its impact on water resources availability in space and time have posed further challenges to the African countries in their aspiration to harness the water and improve food security. In the face of the climate change and deteriorating water availability as the key issues to the sustainability, the shared Africa Water Vision for 2025 and The New Partnership for Africa's Development (NEPAD, 2001) call for the

new ways to assist countries in integrating climate change responses into their national development processes. There are many challenges in the continent in managing water resources with respect to drought, flood and climate change. To explore innovative approaches to meet the challenges, the information on seasonal and annual changes in water resources availability with explicit quantification of blue and green water components in the context of global change is necessary. Achieving such goal with a high spatial and temporal resolution will facilitate design and implementation of climate change adaptation and mitigation measures.

Africa has large disparities in water availability (Schuol et al., 2008). Although water resources are abundant in some regions, water scarcity has been a major constraint to the socio-economic development in many other regions, and the problem will be likely exacerbated in the face of increasing pressure on water supplies due to rapid population growth and dwindling resources (IPCC, 2007). Rain-fed agriculture accounts for 60% of food production. Although irrigated agriculture is a high priority for economic development and stability in most northern and eastern African countries, investment decisions to expand and implement irrigated agriculture is subject to various limiting factors. Among them are economic criteria, upstream–downstream tradeoffs, post-harvest

* Corresponding author. Tel.: +98 311 391 1017; fax: +98 311 391 2840.

E-mail addresses: monireh.faramarzi@cc.iut.ac.ir, faramarzi.iut@gmail.com (M. Faramarzi).

processing facilities, access to markets, policy objectives, and more importantly lack of adequate knowledge and information on the impact of climate change linking biophysical processes and climate factors with irrigation-management factors and planning objectives (You et al., 2010). In the face of climate change, the situation is likely to become more stressed and cause significant economic constraints, negative impact on the livelihood of small holder farmers relying on rain-fed and irrigated agriculture (Odney, 2007). Expanding irrigation, which is identified as a viable adaptive response to climate change (UN Millennium Project, 2005), might not meet the increasing food demand and alleviate poverty (Ziervogel et al., 2006).

Previous studies on climate change in Africa have mainly emphasized the likely impact on rain-fed production and food security in the continent (Thompson et al., 2010; Liu et al., 2008; Thornton et al., 2009; Schlenker and Lobell, 2010; Rowhani et al., 2011). Some studies have addressed changes in hydrology at a river basin scale (e.g. Beyene et al., 2010; Setegn et al., 2011) with focus on particular components, such as stream flow or extreme events (Taye et al., 2011). The climate change adaptation measures in water resources management have also been studied in some individual catchments (Kahinda et al., 2010), or based on qualitative assessments (Krysanova et al., 2010) and reports (Sowers et al., 2011). However, a systematic study, analyzing the impact of climate-induced-scenarios on water resources availability and adaptation strategies on the continental scale with the subbasin as the basic unit of assessment is still missing.

It is widely articulated (Arnell et al., 2004; IPCC, 2007) that climate projections contain significant uncertainties. Many previous studies used ensembles of the climate models and scenarios to characterize uncertainties in the future climate and express the confidence of the impact assessment results (Abbaspour et al., 2009; Tao et al., 2009; Maurer et al., 2009; Kysely and Beranova, 2009; Jinming and Congbin, 2006; Thornton et al., 2009; Gaiser et al., 2011; Semenov and Stratonovitch, 2010). The results show that the individual GCMs as well as the emission scenarios exhibit different biases and show mixed results indicating a substantial sensitivity of GCMs to regional and local processes. These biases are reduced by using ensembles from different GCMs and emission scenarios.

The main objective of this study is to quantify the mid-term impact of climate change on water resources in Africa at a subbasin spatial and monthly temporal scale. This information allows for a better water management and planning of future developments in Africa in the context of climate change. To achieve this goal, we have implemented an integrated hydrological simulation model at the continental level with the subbasin as the basic hydrological unit to study the net effect of climate change on hydrological water balance and water resources components. The time period of the investigation is from 2020 to 2040. This time period was chosen because we are more interested in assessing the impact of climate change on water resources in the near future and also because the lowest fractional uncertainty in climate projections is the future 30–50 years (Cox and Stephenson, 2007). The results will lay the basis for the further analysis of adaptation strategies which will be the subject of a latter study.

We used the Soil and Water Assessment Tool (SWAT) (Arnold et al., 1998) to specifically investigate the impact of climate variability on precipitation and evapotranspiration distribution, river discharge, soil moisture, and aquifer recharge. These variables were then used to quantify the changes in water resources with respect to blue water (i.e. water yield plus deep aquifer recharge) and green water (i.e. soil moisture and evapotranspiration) (Falkenmark and Rockstrom, 2006). The impact assessment was quantified at the subbasin scale using a series of anomaly maps (% deviations from historic data). To quantify the impact of climate

change on water resources availability, we used the ensemble of high-resolution climate data for which outputs of five global climate models (GCMs) have been downscaled and bias-corrected by Mitchell et al. (2004) using the CRU TS 2 dataset of gridded observed data for the period 1961–1990. The dataset comprise all combinations of five GCMs: HadCM3, PCM, CGCM2, CSIRO2, and ECHAM4, and four IPCC emission scenarios: A1FI, A2, B1, and B2 (<http://www.cru.uea.ac.uk>). These GCMs were selected based on data availability to cover a wide range of changes in the global mean temperature. For the SRES scenario A1FI, the CSIRO2 and HadCM3 models can thereby be considered “hot” models with temperature increases of up to 5.5 °C until the year 2100. PCM is rather “cold” with a maximum increase of 3.5 °C until 2100. CGCM2 is in the upper middle with up to 5 °C (Mitchell et al., 2004). The future climate data were then fed to the SWAT model to simulate the changes in different water resources components. In addition, the impact of climate change on the frequency and intensity of floods and droughts was also investigated.

The SWAT model used in this investigation was calibrated and validated previously with uncertainty analysis by Schuol et al. (2008) using SUFI2 algorithm of the SWAT-CUP program (<http://www.eawag.ch/forschung/siam/software/swat/index>). The prediction uncertainty in this hydrologic model reflects the combined uncertainties of input, model structure, and parameters.

2. Material and methods

2.1. The hydrologic SWAT model

SWAT is an integrated semi-distributed hydrological model, which includes a plant growth module. Procedures to describe the effect of CO₂ concentration, precipitation, temperature and humidity on plant growth, evapotranspiration, snow, and runoff generation make the program a valuable tool for the investigation of climate change impacts (Eckhardt and Ulbrich, 2003; Fontaine et al., 2001; Stonefelt et al., 2000). SWAT has been used in many international applications (Gassman et al., 2007) to quantify the impact of land management practices on water, sediment, and agricultural chemical yields in large complex watersheds with varying soils, land uses and management conditions over long periods of time. The model is linked to ArcGIS and therefore capable of analyzing and handling large data sets on various geographical scales. Spatial parameterization of the SWAT model is performed by dividing the watershed into subbasins based on topography, soil, and land use characteristics. The soil water balance equation is the basis of the hydrological model. The simulated processes include surface runoff, infiltration, evaporation, plant water uptake, lateral flow and percolation to shallow and deep aquifers.

In this study, surface runoff was estimated by a modified Soil Conservation Service curve number equation using the daily precipitation data based on soil hydrologic group, land use and land cover characteristics, and antecedent soil moisture. The potential evapotranspiration (PET) was simulated using Hargreaves method (Hargreaves and Samani, 1985). Actual evapotranspiration (AET) was determined based on the methodology developed by Ritchie (1972). The daily value of the leaf area index (LAI) was used to partition the PET into potential soil evaporation and potential plant transpiration. LAI and root development were simulated using the crop-growth component of SWAT, which is a simplified version of the erosion productivity impact calculator (EPIC) crop model (Williams et al., 1984). This component represents the interrelation between vegetation and hydrologic balance. Overall, plant growth was determined from leaf area development, light interception, and conversion of intercepted light into biomass assuming a plant species-specific radiation use efficiency. Radiation use

efficiency is sensitive to atmospheric CO₂ concentrations. Stockle et al. (1992) equations are incorporated in SWAT to adjust radiation use efficiency for effects of elevated CO₂. In addition, climate change can be simulated with SWAT by manipulating the climatic input that is read into the model (precipitation, temperature, solar radiation, relative humidity, wind speed, potential evapotranspiration and weather generator parameters). A more detailed description of the model is given by Neitsch et al. (2005).

2.2. The hydrological model of Africa

We used a previously calibrated SWAT model of Africa based on the studies of Schuol et al. (2008). Data required for this study

consisted of digital elevation model (DEM), land cover map, soil map (FAO, 1995), daily weather input, and river discharge data. Daily climate data were generated from monthly statistics provided by CRU (TS 1.0 and 2.0, <http://www.cru.uea.ac.uk/cru/data/hrg.htm>) at for 0.5° grid points using a semi-automated weather generator, dGen (Schuol and Abbaspour, 2007). The CRU database provides monthly statistics for total precipitation, average minimum and maximum temperatures (Mitchell et al., 2004; Mitchell and Jones, 2005), and the number of wet days per month for each 0.5° grid (New et al., 2000). The grids of the primary variables, precipitation and temperature, are solely based on measured values using an anomalies interpolation technique. Synthetic data estimated from the primary grids were then used in addition to station

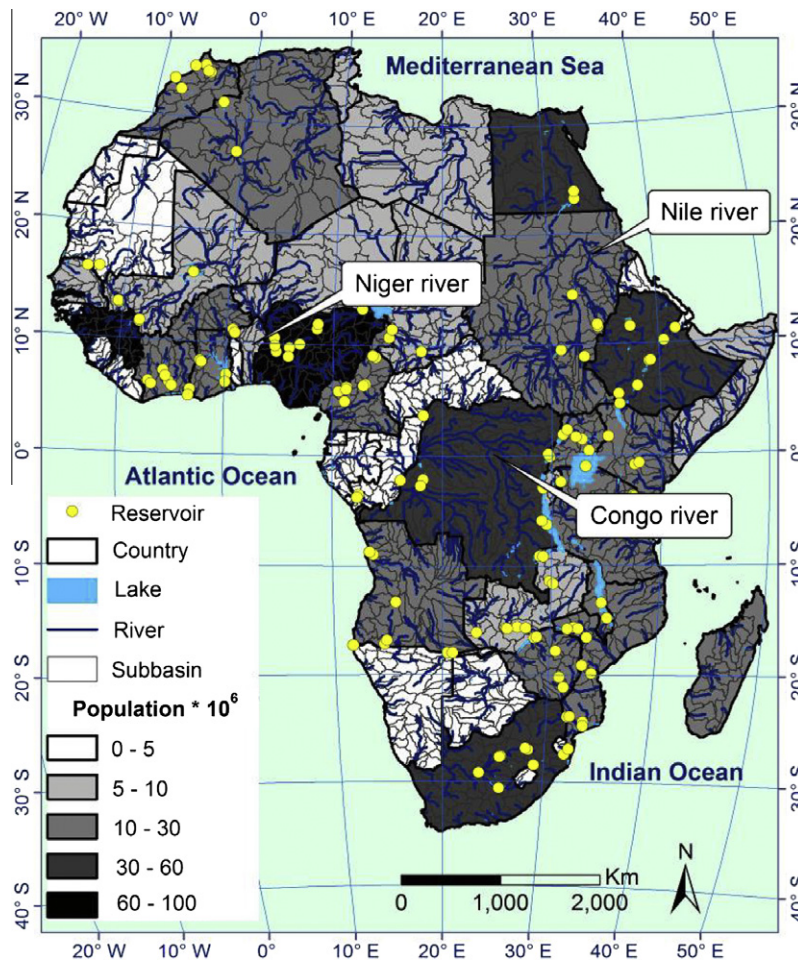


Fig. 1. General map of study area presenting geographic distribution of the rivers, lakes, modeled units (subbasins), political boundaries and country based population (the background color). (For interpretation of the references to color in this figure legend, the reader is referred to the web version of this article.)

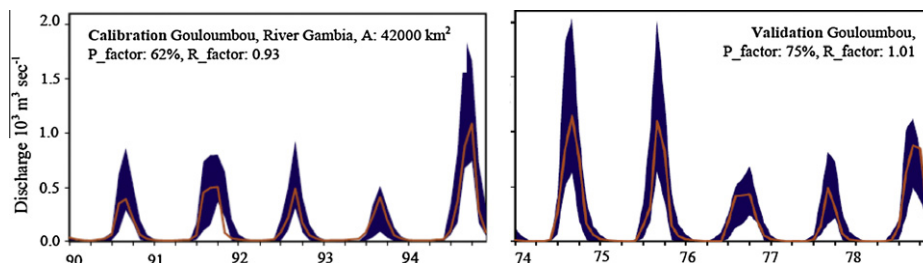


Fig. 2. Results of Soil and Water Assessment Tool (SWAT) calibration–validation for one selected hydrometric station in the arid western part of Africa (adapted from the study by Schuol et al. (2008)).

observations to construct the grids of the secondary variables, like the wet-day frequency.

Based on the input digital maps, a total of 1496 subbasins were delineated and dominant soil and land use were assigned to each subbasin. Based on the availability of data, the simulation period in the model was from 1972 to 1995 (Schuol et al., 2008). Most of the dams, reservoirs and lakes, which affect the river discharge, were included in the model (Fig. 1).

The Sequential Uncertainty Fitting Program (SUFI-2) in the SWAT-CUP package (Abbaspour, 2011) was used for parameter optimization. Using SUFI-2, all sources of uncertainty are mapped to a set of parameter ranges. Two different indices were used to quantify the goodness of calibration–uncertainty performance. These are the percentage of data bracketed by the 95% prediction uncertainty (95PPU) band (*P-factor*) and a measure of the average width of the 95PPU (*R-factor*). In order to compare the measured

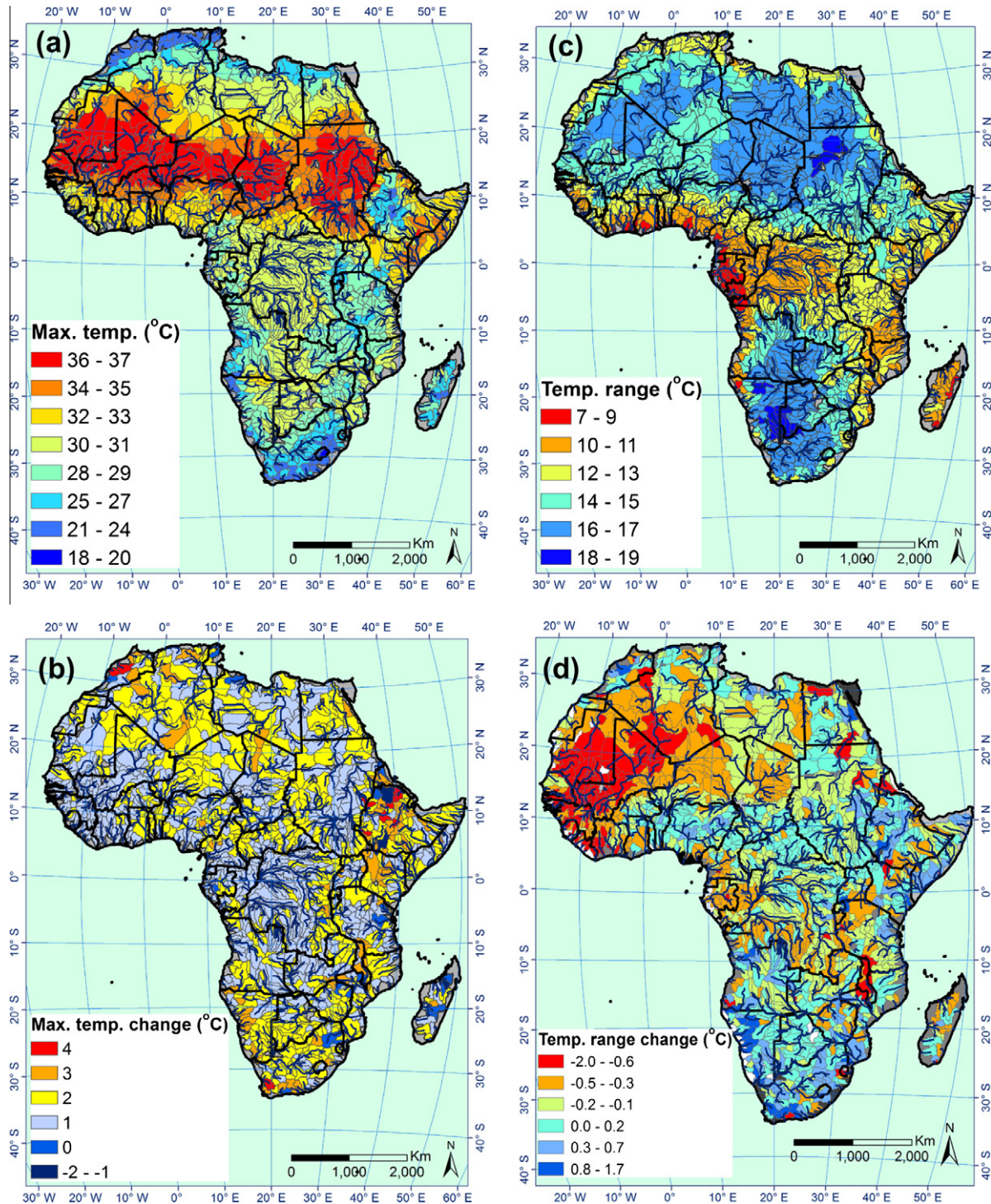


Fig. 3. Spatial pattern of average annual maximum temperature (a) and temperature range which is calculated based on the difference of maximum and minimum temperature (c) for the historic period (1975–1995). Change of maximum temperature (b) and the change of temperature range (d) are shown for the future period (2020–2040) which are based on the predictions of 18 scenarios from five GCMs.

and simulated monthly discharges, an objective function (bR^2 ; where R^2 is coefficient of determination, and b is the slope of the regression line between measured and simulated discharge) (Krause et al., 2005), was optimized based on 207 discharge stations across the modeled area. Overall, the model performance was satisfactory for most of the discharge stations for both calibration and validation period. At 61% of the stations, more than 60% of the observed data were bracketed by the 95PPU and at 69% of the stations the R -factor was below 1.5. The objective function at 38% of the stations was higher than 0.6. Fig. 2 shows the calibration and validation performance of the SWAT model for one discharge station as an example (see Schuol et al., 2008). The calibrated model was then used to account for the subbasin-based and country-based blue and green water resources availability for the study period. More details on the input databases, model setup, and calibration–uncertainty analysis and model results can be found in Schuol et al. (2008).

2.3. The global climate models (GCMs) and emission scenarios

Future climate projections from different models and for various emission scenarios and time periods are provided by the Intergovernmental Panel on Climate Change (IPCC, 2007). In this study we analyzed the hydrological model prognosis for the period of 2020–2040 using 0.5° grids of climate data available through CRU of the University of East Anglia (<http://www.cru.uea.ac.uk>). The set comprises 18 scenarios based on four IPCC emissions scenarios (A1FI, A2, B1, and B2) and five GCMs (HadCM3, PCM, CGCM2, CSIRO2, and ECHAM4) (2000–2100). The scenarios were downscaled by combining time-series of global warming and patterns of change from GCMs with the baseline climate and sub-centennial variability from the observed record. The observed dataset contains monthly observed climate records for minimum temperature, maximum temperature, precipitation and number of wet days for the years 1901–2000 (Mitchell and Jones, 2005).

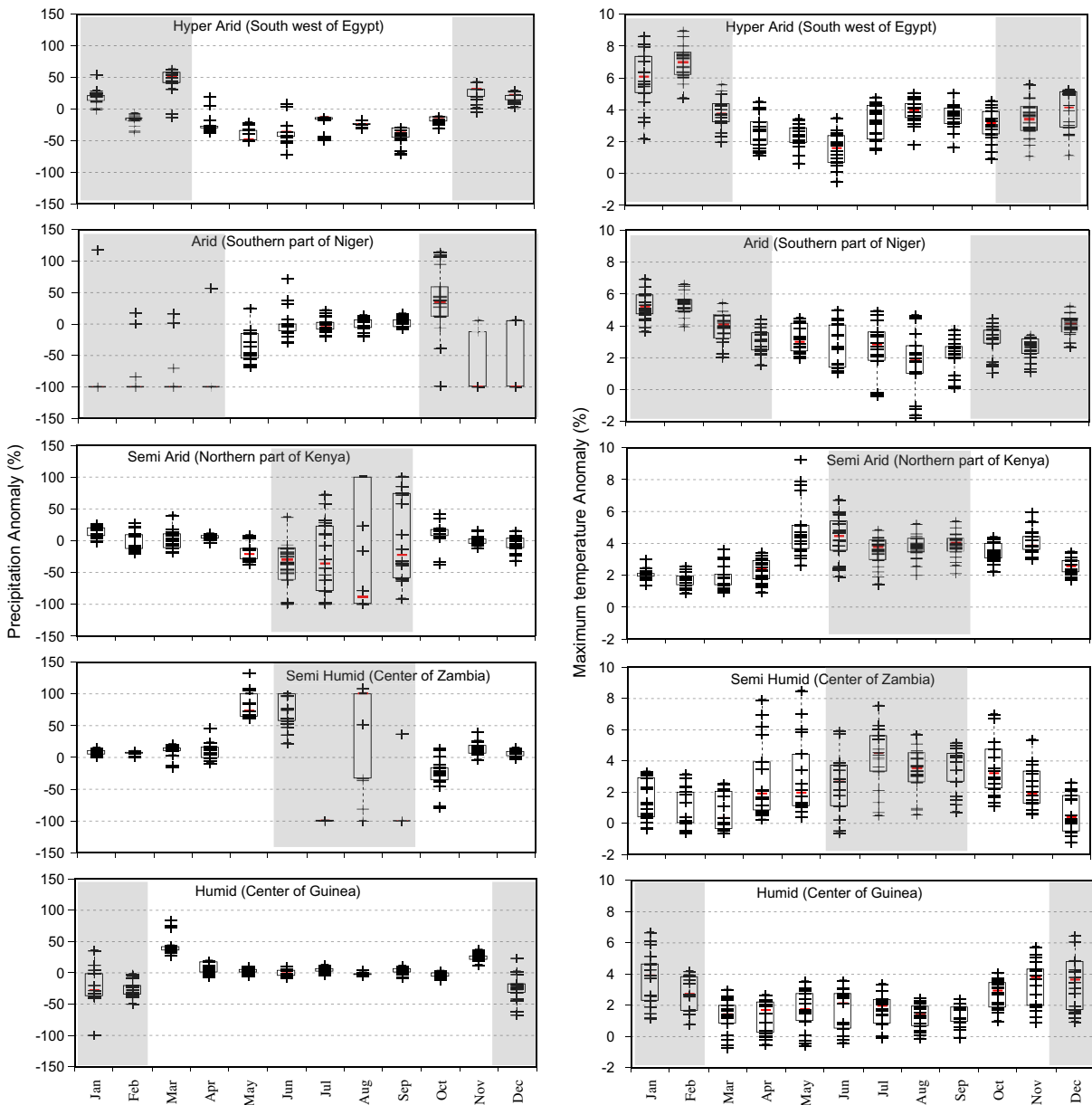


Fig. 4. Projected changes in monthly precipitation and maximum temperature for five selected subbasins from different climate regions (according to Fig. 5) calculated from monthly outputs of 18 different scenarios of five GCMs. The results of different scenarios are shown as pluses, and boxes show the 25th, 50th, and 75th percentiles. The shaded areas in the charts show dry months.

Because the GCMs had a coarser spatial resolution than the 0.5° resolution of the scenarios, a compromise was considered to avoid discontinuities between the 0.5° grid boxes and the influence of ocean GCM grids. Therefore the patterns were interpolated to the 0.5° resolution using a Delaunay triangulation of a planar set of points. Overall, the scenarios were constructed based on four types of information: (i) the baseline climate including observed climatology of 1961–1990 (CRU CL 1.0, 2.0, 2.1) to preserve homogeneity between 20th and 21st century; (ii) the GCMs to represent changes in global climate; (iii) the GCM patterns of climate change at the end of 21st century to express the spatial variability of the GCMs; and (iv) the observed variations in climate during 20th century (CRU TS 1.2, 2.0). With such uniqueness, the 18 climate change scenarios were designed so that they cover 93% of the range of uncertainty in global warming in the 21st century reported by IPCC. The three main sources of uncertainties considered in the dataset were: emission scenarios (68%), climate models (the four GCMs), and internal variability of climate system. The later was partially treated by superimposing the variability of the observed in the 20th century on the mean changes projected for the 21st century to remove the effects of multi-decadal variability. More detail of dataset construction can be found in Mitchell et al. (2004). This dataset does not require a further downscaling or bias-correction for purposes of this study, but as recommended by Mitchell et al. (2004), the climate data could be downscaled for small scale studies where the complex orographic and land–sea distribution may cause local variation in climate change.

The program dGen was also used with the future data to convert monthly statistics to daily values. Based on the dGen algorithm, a wet day was determined by using the popular two state first-order Markov chain. In case of a wet day, the rainfall amount was computed with a two-parameter gamma distribution, and the daily minimum and maximum temperatures were sampled from normal distributions based on monthly averages and standard deviations. The daily climate data were fed into the calibrated and validated hydrologic model of Africa to predict the future impacts on water cycle components. The uncertainty in the hydrological model is represented by parameter ranges (for more detail see Schuol et al., 2008). To capture this uncertainty, 200 sets of hydrologic parameters were obtained using Latin hypercube sampling technique. SWAT was then run with these parameter sets for the baseline climate condition (1972–1995) and the 18 future climate scenarios (2020–2040), resulting in a multi-model-based projection. We set the mean CO_2 concentration for the future to 460 ppm v, 435 ppm v, 425 ppm v, and 400 ppm v under A1FI, A2, B1, and B2 scenarios, respectively (IPCC, 2001). Overall, for each of the 1496 subbasins, 200 parameter sets \times 21 years \times 12 months = 50,400 sets of simulations for 1975–1995 (excluding the first 3 years as warm up period) and 200 parameter sets \times 20 years \times 12 months \times 18 scenarios = 864,000 sets of simulations for 2020–2040 were computed. In each simulation, variables precipitation, water yield, actual evapotranspiration (green water flow), deep aquifer recharge, and soil moisture (green water storage) were extracted from the SWAT output files. Blue water availability was then calculated as water

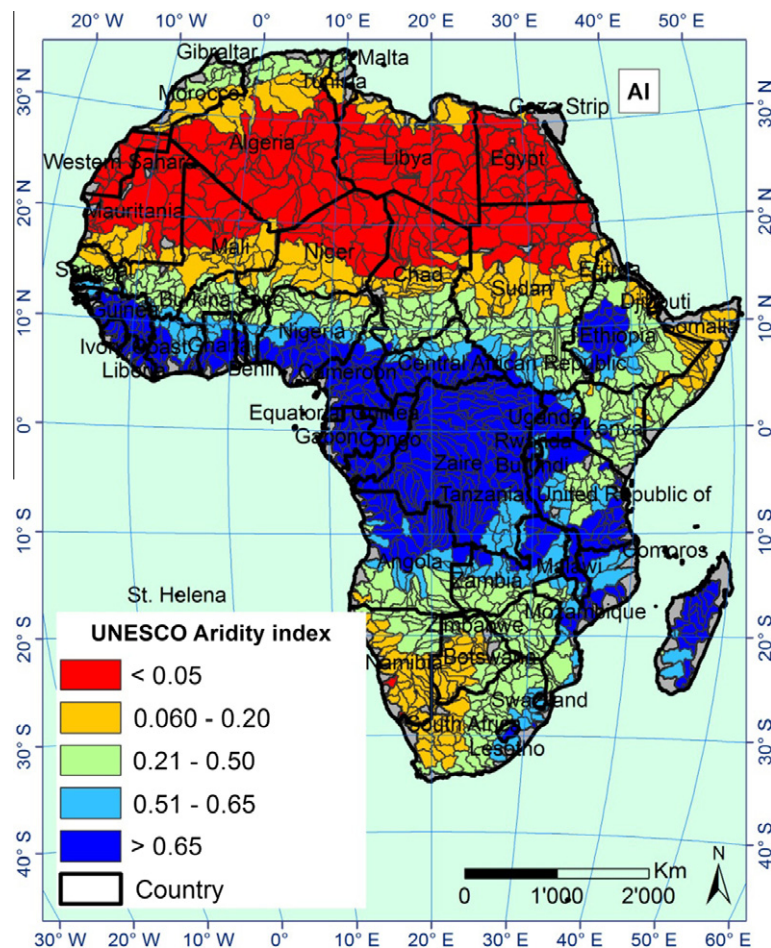


Fig. 5. The average annual (1975–1995) aridity index at subbasin level and for the whole continent. The index is defined as precipitation divided by potential evapotranspiration (UNESCO, 1979). According to this index the boundaries that define various degrees of aridity are defined as: $\text{AI} < 0.05$: hyper-arid, $0.06 < \text{AI} < 0.2$: arid, $0.2 < \text{AI} < 0.5$: semi-arid, $0.5 < \text{AI} < 0.65$: semi-humid, $\text{AI} > 0.65$: humid.

Table 1
Median of the projected changes of monthly precipitation in five selected subbasins from different climate regions. The shaded areas show dry seasons.

Climate region	Jan	Feb	Mar	Apr	May	Jun	Jul	Aug	Sep	Oct	Nov	Dec
Hyper-arid (Egypt)	19.23	-14.52	50.51	-28.48	-49.25	-36.56	-13.55	-23.67	-38.42	-14.15	30.52	21.46
Arid (South Niger)	-100.00	-100.00	-100.00	-100.00	-47.90	-4.60	-5.83	2.72	-0.02	33.52	-100.00	-100.00
Semi-arid (North Kenya)	9.59	-8.82	-0.81	5.73	-21.69	-29.42	-36.67	-89.14	-23.19	15.22	-2.07	-6.76
Semi-humid (Zambia)	8.97	7.11	12.62	11.21	73.64	76.35	-100.00	100.00	-100.00	-23.12	9.45	7.63
Humid (Guinea)	-28.90	-27.73	38.79	6.88	4.58	-1.95	2.76	-3.60	2.39	-4.31	22.97	-24.64

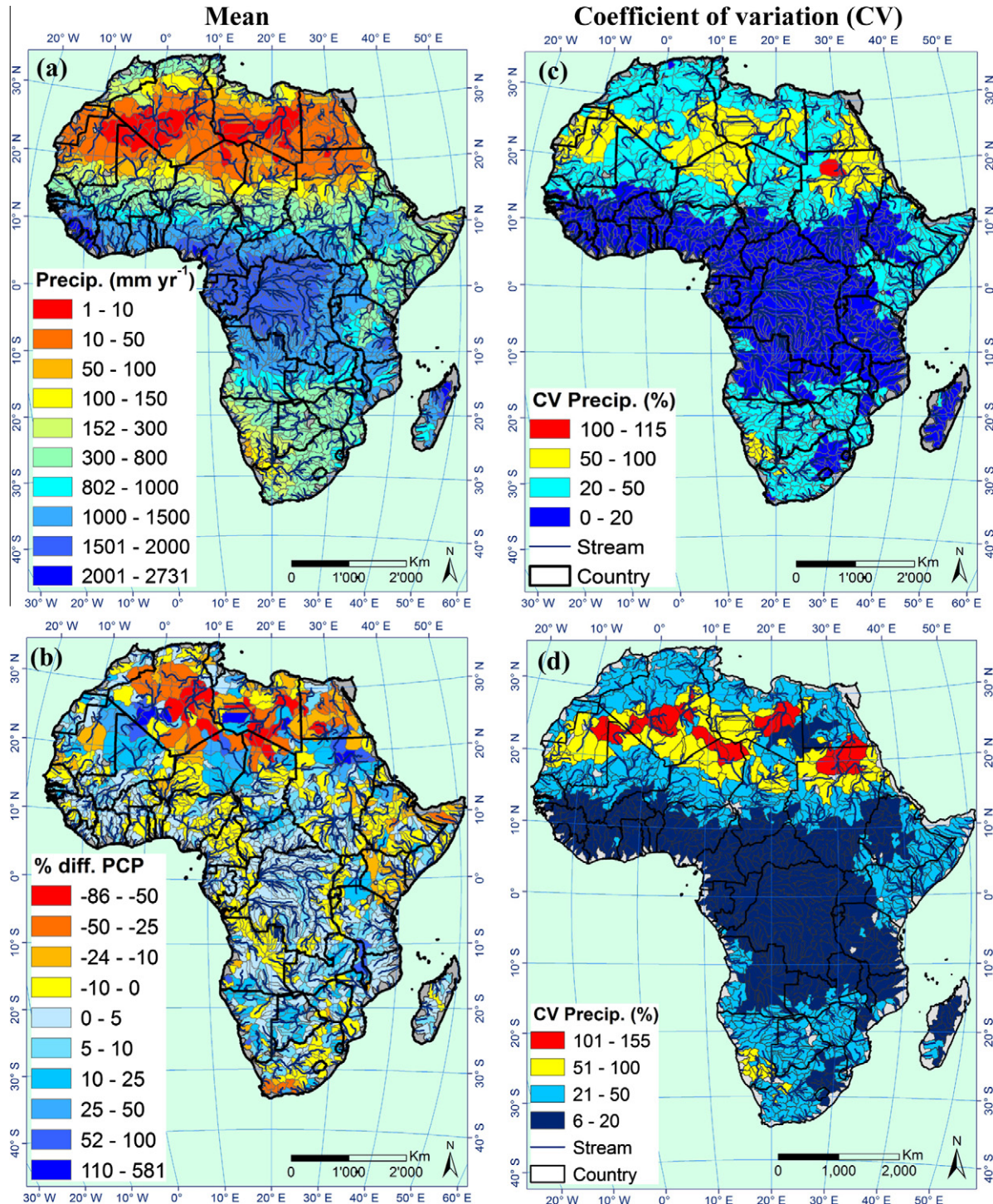


Fig. 6. Spatial pattern of mean (a) and coefficient of variation (c) of precipitation during 1975–1995 period, and anomaly map of the precipitation which is the % difference calculated based on the data period 2020–2039 from the 1975 to 1995 (b), and coefficient of variation during 2020–2039 (d). The predictions of 18 scenarios from five GCMs were considered in the future calculations.

yield plus deep aquifer recharge. We used the SUFI-2 program to calculate the simulation results at the 2.5%, 50%, and 97.5% probability levels. The simulation results at the 2.5% and 97.5% levels were used to calculate the 95% prediction uncertainty band (95PPU) and the results at the 50% level was used to calculate the changes in the variables relative to the corresponding historic simulations during 1975–1995.

3. Results

3.1. Impact of climate change on temperature and precipitation

The historic distribution of average maximum temperature (Fig. 3a) ranges from 18 to 37 °C across the continent. The changes in maximum temperature (Fig. 3b) in most subbasins of the continent, as a result of climate change, are between 1 and 3 °C. Most of West and Central Africa is seen an increase of about 1° in temperature while in South and North Africa the increase is mostly about 2°. The anomalies are calculated as the % differences between the prediction uncertainties of the 18 climate scenarios at the 50% probability level and averaged over the period of 2020–2040 and those of the historic (1975–1995) period.

The diurnal temperature range shown in Fig. 3c is the historic difference between maximum and minimum temperatures. The difference is 7–19° across Africa. This difference narrows by –2 to 0 °C in most of North Africa (Fig. 3d) and widens by about 0–1.7 °C in the Central and Southern Africa. This implies that

minimum temperature increases faster in North and Central Africa and slower or even decreases in most of Southern Africa.

Five selected subbasins (Fig. 4) were chosen from different climatic regions based on the aridity index of UNESCO (1979). For this, different aridity levels were calculated for the study area (Fig. 5). In all climate regions from hyper-arid to humid, the maximum temperature increases in most months for all the climate scenarios (Fig. 4). The temperature increase in all climate regions is larger in the dry seasons, implying that regions already suffering from drought may face even bigger challenges in the future. In the semi-arid region (particularly subbasins in the horn of Africa) where temperature shows a larger increase in the wet months, a likely decrease in precipitation is projected (Fig. 4, and Table 1). Similar to temperature, precipitation showed an increasing pattern in most of the wet months in humid and semi-humid regions while it decreased by about 48% in the wet months of hyper-arid and arid regions respectively (Table 1). It is worth mentioning that the projected changes of precipitation from different climate scenarios were more consistent in wet months than dry months (smaller width of the box plots in Fig. 4). A larger disparity in the predictions for dry months is partly related to the propagation of the calculation error when accounting for “percent difference” from the historic. Where historic values are very small and close to zero, a large percentage difference is obtained with a small over or under projection (larger width of the box plots).

The historic precipitation (Fig. 6a) and precipitation change (Fig. 6b) is different from subbasin to subbasin, but a general pattern is observed for the whole continent. Looking at the Northern

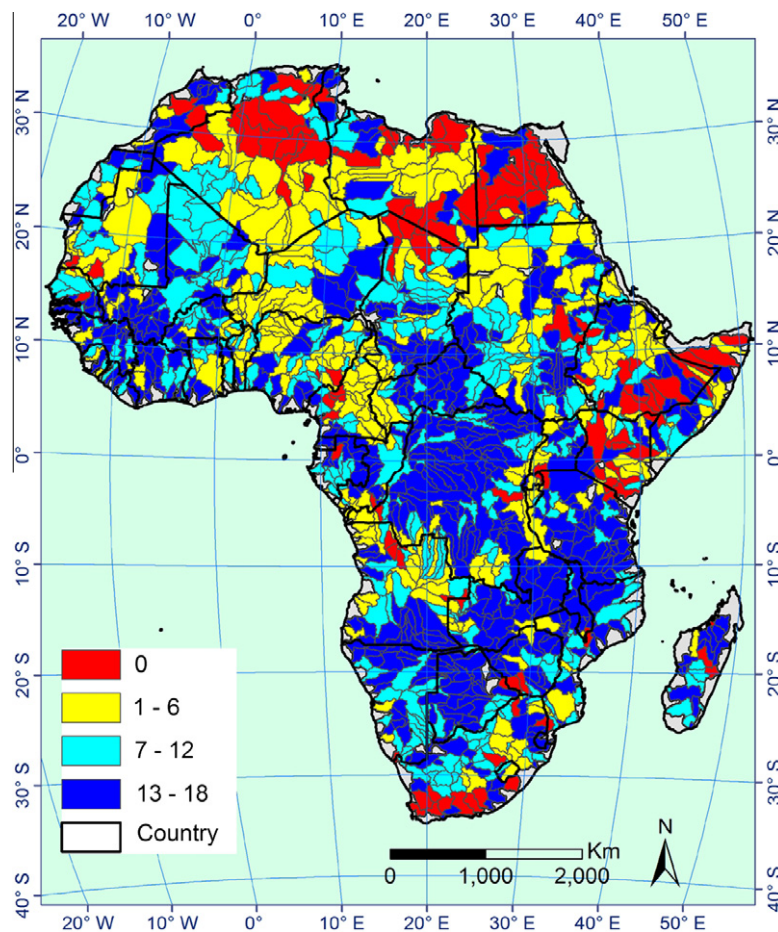


Fig. 7. Number of scenarios predicting increase of more than 1% for precipitation compare to the historic period. Any change between $\pm 1\%$ are considered as unchanged situation.

segment of the continent, the countries which are already experiencing hyper-arid conditions like Egypt, Libya, Algeria, and Western Sahara will be even more stressed with a decrease in precipitation by 25–50%. Comparison of the annual variation for the two periods (Fig. 6c and d) shows that in the northern hyper-arid region, the coefficient of variation could reach as high as 100–150% indicating severe fluctuations in the year to year precipitation amount. This may have a significant effect on increasing

prolonged droughts and hence crop production in these countries. Other prominent regions receiving up to 25% more rainfall are located mostly in southwest Africa (e.g. Namibia, Botswana, Zaire, Zambia) and western Africa (i.e. coastal areas such as Guinea and Ivory coast). The situation is reversed in the southern part of South Africa, northern part of Angola, northern Cameroon in the West Africa, and Ethiopia, Somalia and Kenya in the Horn of Africa, where precipitation could decline by up to 25%.

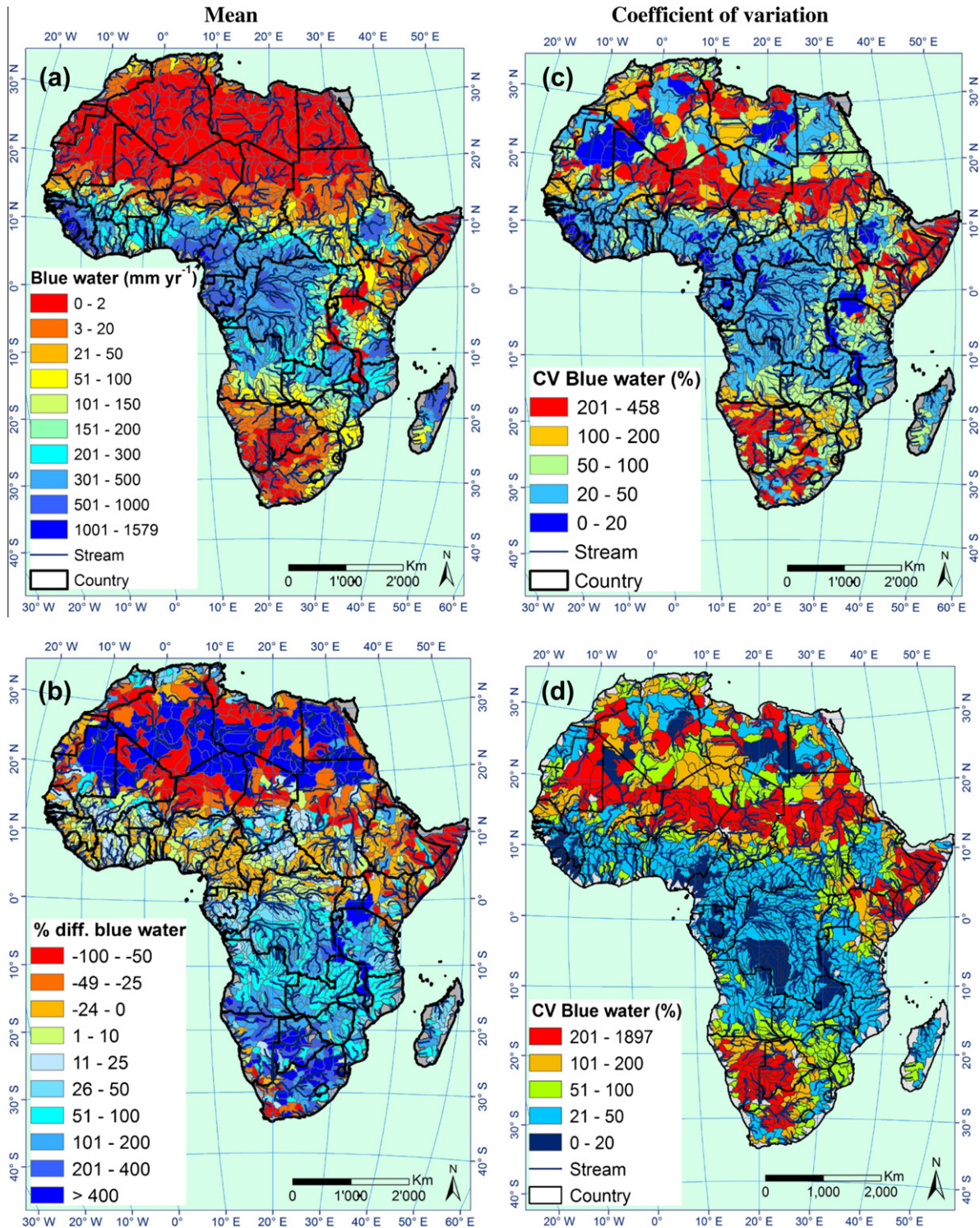


Fig. 8. Spatial pattern of mean (a), and coefficient of variation (c) of blue water resources which are calculated based on the average annual M95PPU (i.e. 50th percentile out of 200 simulations) values during 1975–1995 period, anomaly map which is the % difference calculated based on the data period 2020–2039 from the 1975 to 1995 (b), and coefficient of variation of blue water during 2020–2039 (d) for which the predictions of 18 scenarios from five GCMs are considered.

To assess the reliability of our projection results we constructed Fig. 7 to show the number of the climate scenarios with a similar projection results. While the temperature projections from the 18 climate scenarios were quite similar across Africa (figures are not shown), the projected patterns of precipitation varied considerably from scenario to scenario. In the subbasins depicted with blue color, 13–18 climate scenarios predicted an increase of more than 1% in the rainfall for the central and western Africa. In the yellow subbasins only 1–6 out of 18 climate scenarios predict an increase of more than 1% for the rainfall. Hence, more confidence could be placed on the blue subbasins.

3.2. Impact of climate change on freshwater components

In the literature, the term “blue water” refers to the summation of the water yield and deep aquifer recharge which are renewable resources. Green water flow is defined as the actual evapotranspiration, and green water storage is the soil moisture (Falkenmark and Rockstrom, 2006). Fig. 8a shows the average values of blue water (mm yr^{-1}) based on the historic data of 1975–1995. The projected effects of climate change are shown in Fig. 8b as the anomaly map based on the averages of the prediction from the 18 climate scenarios. Generally, blue water will increase in the southern part of the continent except in the very dry southern border and south west coastal areas of South Africa and Namibia. An increase of up to 400% in these regions, however, might not bring a significant increase in blue water resources availability because of the very low basis. The countries located in the Horn of Africa and Sahel will suffer from a decrease of blue water resources by 25–100%. Fig. 8c illustrates the coefficient of variation of the historic blue water resources. Blue regions are more reliable in terms of their water resources from year to year. Comparison of the historic coefficient of variations of blue water resources with that of the future (Fig. 8d) shows that inter-annual change of blue water resources availability is more or less similar to the past in most of the central and northern parts while an increase in southern semi-arid and arid areas is observed, implying less reliability in the blue water increases in these regions.

We aggregated the subbasin-based predictions of blue water resources to the country level (Fig. 9). For most countries, the average future prediction is larger than the lower bound of the historic

prediction uncertainty. The future blue water resources availability in 20 countries is larger than the upper bound of our hydrologic model prediction for the historic situation. Hence, a larger confidence could be put on the blue water increases in these countries (Table 2). Taking the blue water resources at the 50% probability level resulted in 34 countries gaining more blue water in the future. In countries (i.e. shaded cells in Table 2) where both L95PPU and U95PPU point to the same conclusion, the results will be more reliable for future management and planning. In contrast in the countries where future water resources is just greater than the lower bound of the prediction, such as Burkina Faso, Cameroon, Congo, Chad, Ethiopia, Guineas, and Sudan, the projection results should be viewed with more caution.

There are significant spatial variations in the long-term average annual green water storage (soil moisture) (Fig. 10). Southern part of Africa shows an increase in soil water with a larger reliability than the blue water resources. Although a larger soil moisture is predicted (Fig. 10b), its reliability is quite low (Fig. 10d).

To give a clear picture of the relationship between projected changes of all hydrological components, we included also the maps of actual and potential ET as well as deep aquifer recharge (DARCHG) with their possible changes in the future (Fig. 11). The changes in AET (Fig. 11a and d) are consistent with the changes in PET (Fig. 11b and e) in most parts of the study area except the northern hyper-arid to arid regions and south western countries (i.e. Namibia and Botswana). In the regions where the deep aquifer recharge is historically small (i.e. the very south and northern parts of the continent), even a large percentage increase (Fig. 11c and f) would not improve the water supply situation. In contrast, in the central part a considerable increase of deep aquifer recharge is projected, which is consistent with the increase of green water storage (Fig. 10a and b). This region will also enjoy abundant blue water resources in the future. A considerable decrease of deep aquifer recharge is projected for West Africa. As expected, it is in agreement with the decline of blue water resources.

3.3. Impact of climate change on the duration of dry and wet periods

To investigate the impact of climate change on flooding and drought we selected seven subbasins from different climatic conditions in Africa and calculated the average distribution of the

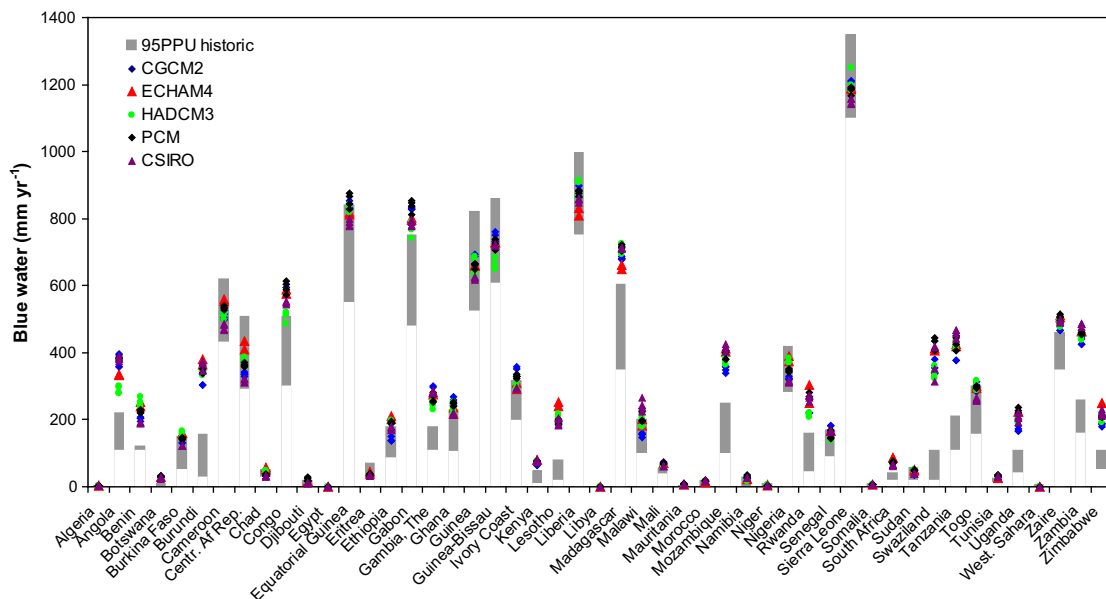


Fig. 9. Comparison of the SWAT 95PPU ranges of the annual average (1975–1995) blue water availability in the African countries with that of 18 scenarios of the five GCMs for the period 2020–2039. In this figure the average annual M95PPU values are presented for each scenario.

Table 2

Comparison of the historic and projected range of country-based blue water availability (BW) considering the L95PPU and the U95PPU value of the annual average (1975–1995) blue water values. Shaded cells indicate the countries where both L95PPU and U95PPU of the historic BW values led an increase of BW for all scenarios in the future period. The right column shows the range of the projected BW from 18 scenarios.

Country	Historic BW L95PPU (mm yr ⁻¹)	Historic BW U95PPU (mm yr ⁻¹)	Future BW M95PPU (mm yr ⁻¹)
Algeria	0	4	2–3
Angola	110	220	277–396
Benin	110	120	187–267
Botswana	0	10	22–32
Burkina Faso	50	150	120–167
Burundi	28	158	303–381
Cameroon	430	620	465–559
Centr. Af Rep.	290	509	310–434
Chad	28	50	30–57
Congo	300	509	485–614
Djibouti	0	20	10–29
Egypt	0	0	0–0
E-Guinea	550	840	776–875
Eritrea	30	70	33–43
Ethiopia	85	180	136–210
Gabon	480	750	740–854
Gambia	110	180	231–300
Ghana	107	230	213–267
Guinea	525	820	616–692
Guinea-Bissau	608	860	649–761
Ivory Coast	198	318	291–358
Kenya	10	48	65–81
Lesotho	20	79	181–253
Liberia	750	997	807–914
Libya	0	1	0–1
Madagascar	350	604	647–727
Malawi	100	200	148–264
Mali	38	53	58–73
Mauritania	0	4	4–10
Morocco	0	20	14–20
Mozambique	100	248	340–426
Namibia	0	30	15–34
Niger	0	10	2–5
Nigeria	280	420	309–391
Rwanda	45	160	209–305
Senegal	90	170	137–183
Sierra Leone	1100	1350	1142–1251
Somalia	0	10	6–7
South Africa	18	43	61–87
Sudan	20	58	35–52
Swaziland	20	110	313–444
Tanzania	110	210	378–468
Togo	158	300	257–317
Tunisia	13	26	26–34
Uganda	40	110	167–235
W-Sahara	0	5	0–0
Zaire	350	460	466–515
Zambia	160	260	426–485
Zimbabwe	50	110	180–249
Africa	118	161	140–232

number of days with precipitation >2 mm d⁻¹ and precipitation >10 mm d⁻¹ for these regions during 1975–1995 and 2020–2040 (Fig. 12). Most scenarios indicate that the hyper-arid region of southwestern Egypt (Fig. 12a and b) as well as the semi-arid region of northern Kenya (Fig. 12e and f) experience larger number of days with precipitation >2 mm d⁻¹ in spring months. This is true for the summer months of the arid region of southern Niger (Fig. 12c and d). In the arid regions of South Africa, the northern region shows the largest increase in the number of wet days in winter and spring months for both >2 and >10 mm d⁻¹ rainfall events (Fig. 12k and l). This is corroborated by all scenarios. In the southern parts of South Africa (Fig. 12m and n), all scenarios indicate a decrease in the number of days with precipitation >2 mm d⁻¹ in

the winter and spring months, along with an increase in the summer months.

In humid and semi-humid regions, the number of wet days is projected to increase in most of the months (Fig. 12g–j). The number of days with larger rainfalls, precipitation >10 mm d⁻¹, is not increased significantly in both humid and semi-humid regions. However, the small changes in the number of wet days in the arid and semi-arid regions are unlikely to bring about important consequences to water conditions.

In a further analysis we plotted Fig. 13 to show the coefficient of variation (CV) of the number of wet days per year for precipitation >2 mm d⁻¹ (Fig. 13a) and precipitation >10 mm d⁻¹ (Fig. 13b). In general, the CV of the number of wet days in hyper-arid region (Egypt) is significantly larger than that of other climate regions, mainly due to a very small mean value. Therefore, we divided the CVs of this region by 10 to be able to show it within the same chart as the other regions. A substantially large increase in the CV in hyper-arid (Egypt) and dry region of South Africa for the number of days with rainfalls >2 mm d⁻¹ and rainfall >10 mm d⁻¹ imply a stronger year-to-year variation in these areas. The rest of the regions show either no change or small changes compare to the historic period.

To demonstrate the severity of the dry periods in Africa, we calculated the number of consecutive days with rainfall <2 mm d⁻¹. Fig. 14 shows the recurrence times and the average length of dry periods. The numbers of such periods were counted for the duration of 20 years in the past (1975–1995) and the future (2020–2040) using all 18 scenarios and then averaged. In general, the duration of dry periods increases in the future in the north and in the south, while the central Africa and regions in southeast experience shorter duration of dry periods.

4. Discussion

4.1. Comparison of this study with the literature

There are many published works on the trend of temperature and rainfall as well as water availability and extreme events concerning drought and flooding under the future climate change in Africa. Substantial variations exist across different climate scenarios. In general, projected changes in precipitation and dryness extremes are more ambiguous than those in temperature extremes (Orlowsky and Seneviratne, 2012).

Most researchers have projected the temperature increase of Africa between 2 and 4 °C (e.g. Boko et al., 2007; Agoumi, 2003). CEEPA (2006) published a working paper reporting the results of assessment of possible impacts of climate change for the whole continent. The study derived 16 scenarios using five different GCMs (CSIRO2, HadCM3, CGCM2, ECHAM and PCM) based on two different emission scenarios (A2 and B2). The results for decadal average changes for 2050 and 2100 in annual values for precipitation, temperature and stream flow are presented. For temperature, they show a range of increase of 2.2–4.1 °C for most of Africa. In this study, we also generally projected an increase of 1–4 °C in most of the continent with larger increases in the northern part of the continent (2–4°) and smaller increases in mid-continent (1–2°).

Ruelland et al. (2012) used the climate models HadCM3 and MPI-M under SRES-A2 to provide future climate scenarios in a large Sudano-Sahelian catchment in Africa. Outputs from these models were used to generate daily rainfall and temperature series for the 21st century. A temperature-based formula was used to calculate present and future potential evapotranspiration (PET). The daily rainfall and PET series were introduced into the calibrated and validated hydrological model to simulate future discharge.

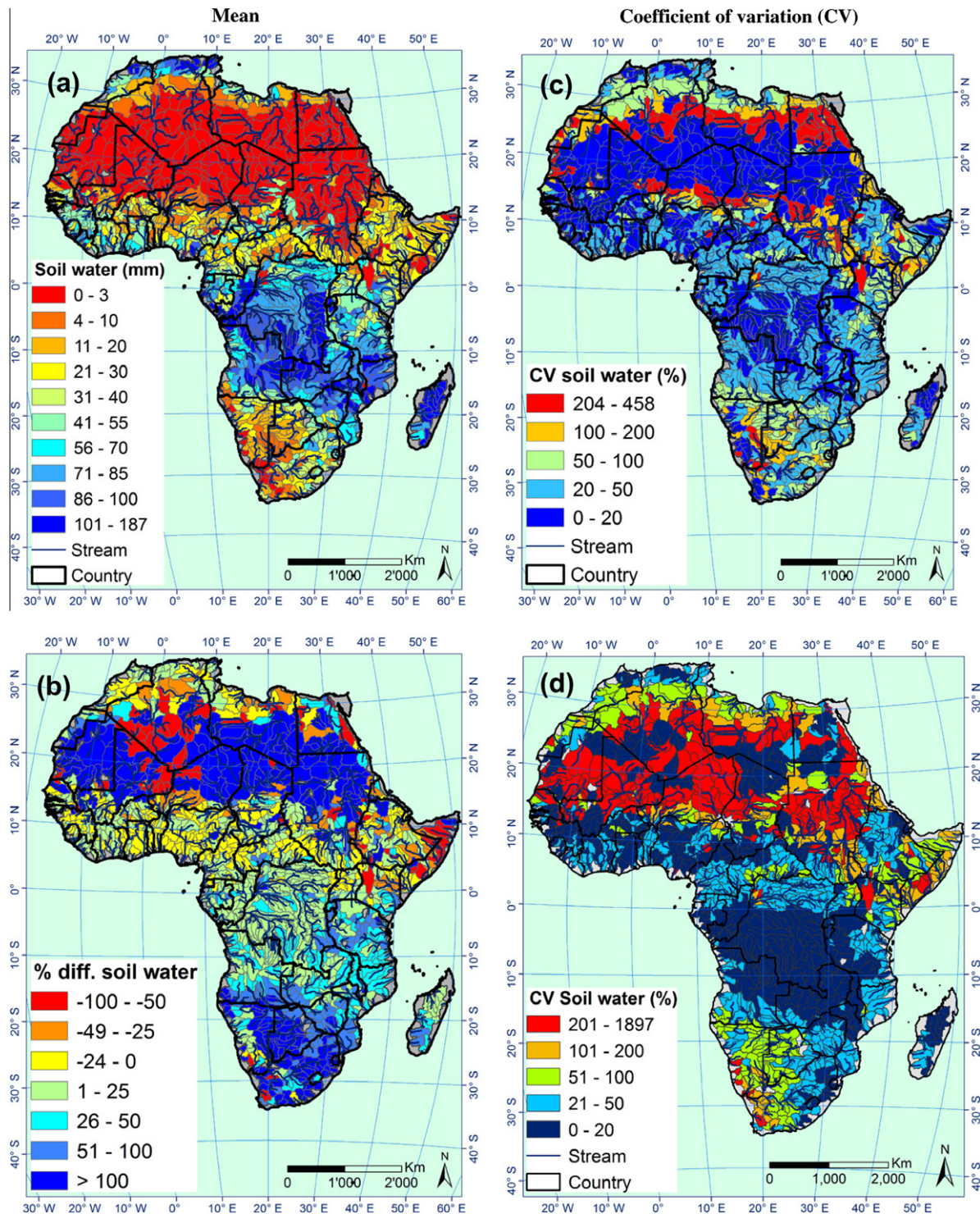


Fig. 10. Spatial pattern of mean (a), and coefficient of variation (c) of green water storage which are calculated based on the average annual M95PPU values during 1975–1995 period, anomaly map which is the % difference calculated based on the data period 2020–2039 from the 1975 to 1995 (b), and coefficient of variation of soil water during 2020–2039 (d) for which the predictions of 18 scenarios from five GCMs are considered all together.

With regard to future climate, the results show clear trends of reduced rainfall over the catchment. This rainfall deficit, together with a continuing increase in potential evapotranspiration, suggests that runoff from the basin could be substantially reduced, especially in the long term (60–65%), compared to the 1961–1990 reference period. As a result, the long-term hydrological simulations show that the catchment discharge could decrease to the

same levels as those observed during the severe drought of the 1980s. Our study shows large variability in future rainfall distribution within the catchment; where rainfall decreases toward the eastern part of the catchment and increases in the north.

Regional variations in precipitation are substantial (Fig. 6). Shongwe et al. (2009) report a general increase in rainfall in the tropics, which is also the case in this study. In East Africa they

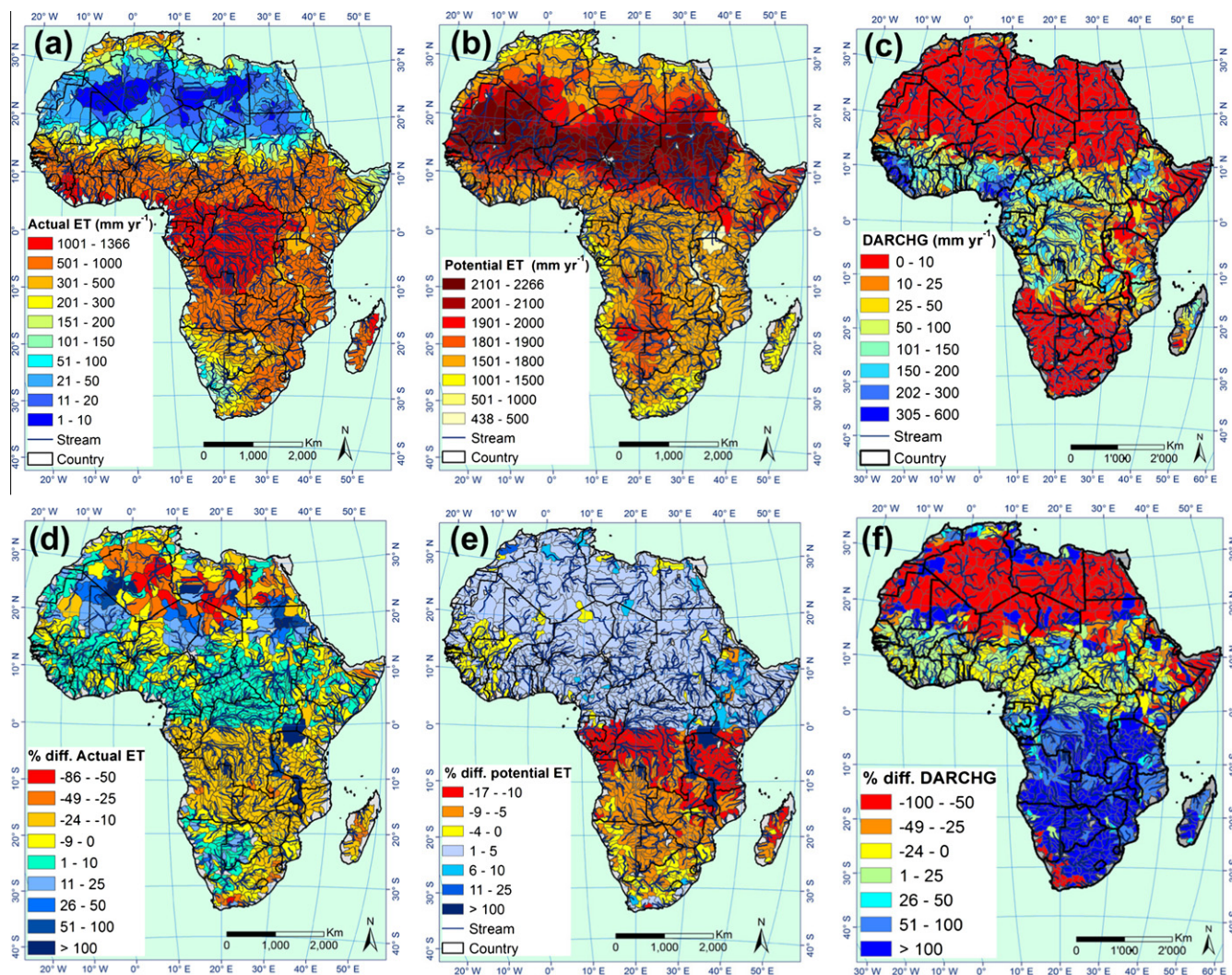


Fig. 11. Spatial pattern of actual ET (a), Potential ET (b) and deep aquifer recharge (c) which are calculated as the averages of the annual M95PPU values during 1975–1995 period, and anomaly maps which are the % differences calculated based on the data period 2020–2039 from the 1975 to 1995 (d–f).

report a generally wetter climate. However, our study indicates a large spatial variation from a decrease of 25–50% to an increase of 25–50%.

The **CEPA (2006)** report shows a range of changes in rainfall of –13% to 57% for different countries across the continent with large variations between countries in different parts of Africa. Our sub-basin-based calculations projected mostly consistent patterns although with a large variation within each country (Fig. 6).

Andersson et al. (2011) in their study of the Pungwe river basin in Mozambique using ECHAM4 (A2, B2 scenarios) and CCSM3 (B2 scenario) report a 10% reduction in rainfall. Our study, however, shows a large variability in rainfall within the country. **de Wit and Stankiewicz (2006)** conducted an assessment of the relationship between rainfall and discharge across Africa. They found that a 10% decrease in precipitation in regions on the upper regime boundary (1000 mm per year) would decrease surface drainage by 17%, whereas in regions receiving 500 mm per year, such a drop would cut 50% of drainage. By using predicted precipitation changes, they calculated that a decrease in perennial drainage will significantly affect present surface water access across 25% of Africa by the end of this century. In general, North Africa, the Saharan Region, and southern Africa are the regions with decreases in discharges of between 10% and 20% and the central Africa and East

Africa are projected to have increase in discharge between 10% and 20%. Our estimation of blue water availability shows a generally similar trend but with significant spatial variabilities.

In the **CEPA (2006)** report, most countries show a decrease in stream flow, while our model estimates a generally net increase in blue water resources for most countries (Figs. 8 and 9). However, there are large variabilities within each country. An advantage of our sub-basin-based analysis is that these spatial variabilities are highlighted. For example, some subbasins within the Saharan Region show increase of up to 400% in blue water availability, albeit these increases are still quite small. In the study by **Murray et al. (2012)**, runoff increase is projected in the Congo river basin for the period 2070–2099 over the period 1961–1990 under a 2 °C (by 2050) increased warming scenario, based on the averages of six GCM simulations. This is also evident in our study (Fig. 9).

Dai (2011) provided a comprehensive review of the projected drought situation under global climate change. The study found that climate models mostly projected increased aridity in the 21st century over most of Africa. Although aridity is not well defined in this report, it interpreted as longer and more frequent dry periods. This is also what we found (Fig. 14). Report of worsening drought situation is also predicted by **Andersson et al. (2011)**.

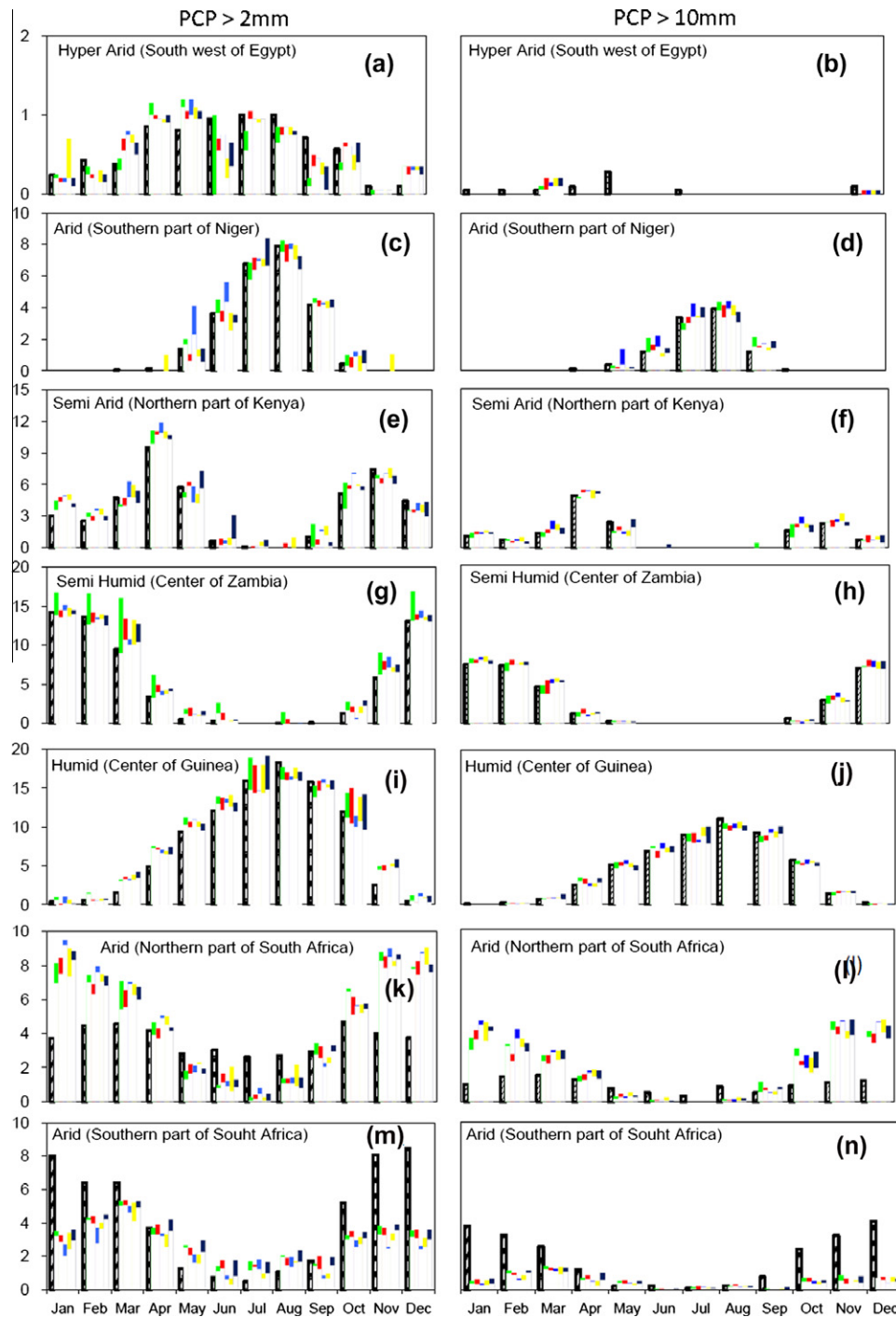


Fig. 12. Comparison of the number of wet days between historic (1975–1995), presented with dashed columns and future (2020–2039) periods for subbasins selected from different climatic regions according to the aridity map of Fig. 5. The colored bands show the range of predictions resulted from different scenarios in each GCM (CGCM2: green, CSIRO: red, ECHAM: blue, HADCM3: yellow, PCM: black). In these graphs a wet day is defined as a day with precipitation >2 mm (left column), and >10 mm (right column).

4.2. Implication of changes in rainfall, green and blue water, and actual evapotranspiration

One objective of this study was to compare the consistency of the projected changes in different water balance components at the subbasin scale. It is widely discussed in the literature that the stream flow and the blue water resources in general are sensitive to rainfall (Faramarzi et al., 2009; Setegn et al., 2011; Schuol et al., 2008). This is in agreement with our findings in most of

the areas, except some subbasins (e.g. in the southern part of South Africa) where a decrease of precipitation (Fig. 6b) led to an increase in blue water (Fig. 8b) and soil moisture (Fig. 10b). The reason is that in these subbasins, the PET, and subsequently, the AET (green water flow) decreases (Fig. 11) so that most of the rainfall contributes to the blue water and soil moisture as simulated by the SWAT model. A major reason for the decrease of PET in these regions is the decrease in surface air temperature, which is effective in the calculation of PET using the Hargreaves method.

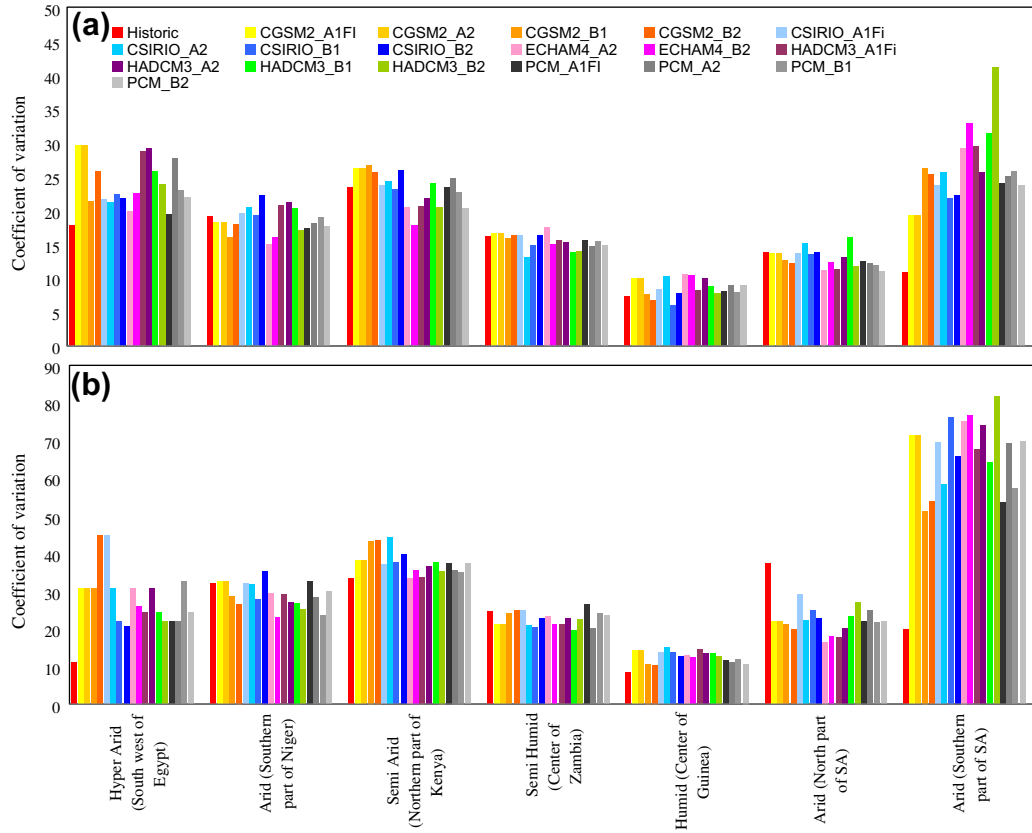


Fig. 13. Coefficient of variation of the number of wet days. Shown are (a) precipitation $>2 \text{ mm d}^{-1}$ and (b) precipitation $>10 \text{ mm d}^{-1}$, for the selected subbasins in different climate regions of continent of Africa. The presented columns in Figure b for the hyper-arid (south west of Egypt) are divided by 10 to equalize the scale.

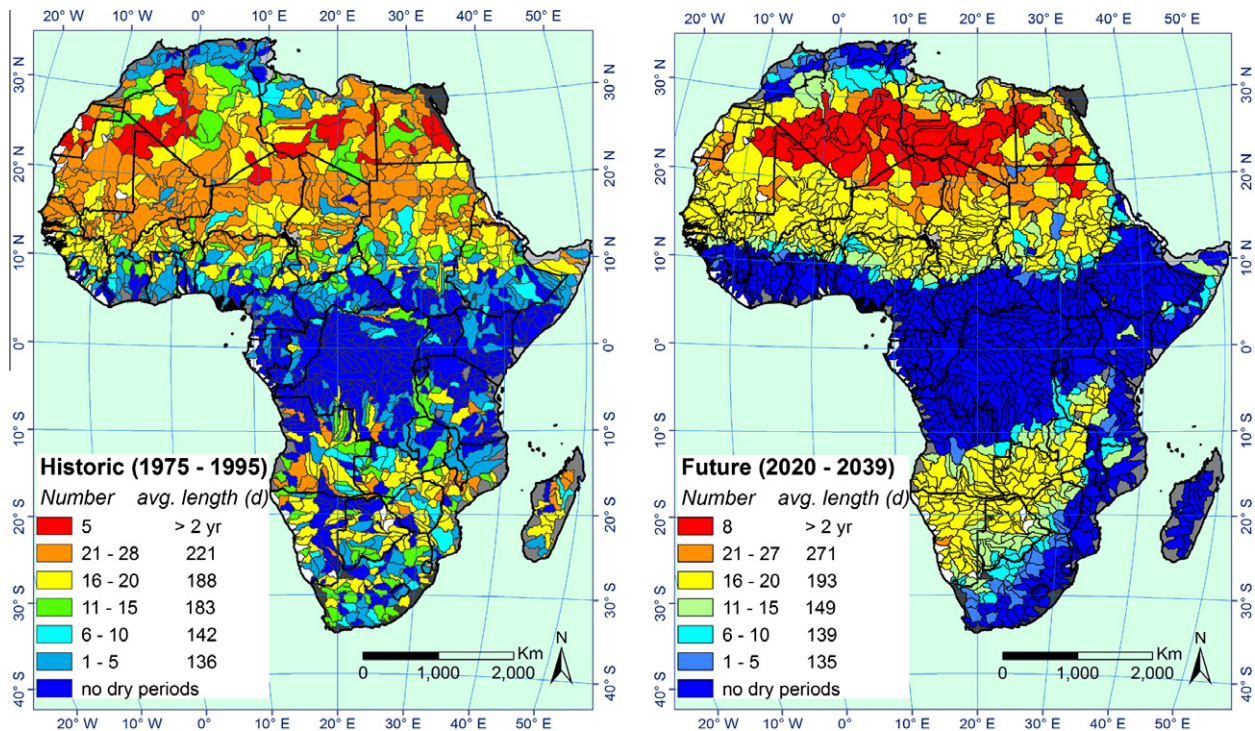


Fig. 14. Comparison of the number of drought events (left column in the legend) and the average drought length (right column in the legend) for historic and future scenarios.

As shown in Fig. 11, the changes in AET (Fig. 11a and d) is consistent with the changes in PET (Fig. 11b and e) in most parts of the study area except the northern hyper-arid to arid regions and

south western countries (i.e. Namibia and Botswana). The main reason for this difference is that a small decrease in PET (i.e. 10%) will still impose a large evaporative demand ($1350\text{--}1680 \text{ mm yr}^{-1}$)

in these regions. Lesser constraints in precipitation (Fig. 6b) and soil water storage (Fig. 10b) enable the region to meet more of the high evaporative demand. In other words, small changes in PET along with an increase in CO₂ levels can trigger significant changes in AET. This is because plants grow more vigorously with increasing temperature and CO₂, as the rainfall and subsequently soil moisture increases.

In Africa, climate change will lead to increase in climatic variability and decrease in blue and green water resources. These changes and spatial variations will exert significant impacts on the economic development, particularly for the agricultural and water-resources sectors, at regional and local scales. In semi-arid regions of the Sahel, Horn of Africa, and Southern part of Africa, large rural and urban communities depend on water availability for rain-fed agriculture, as well as biomass derived energy. Climate change is expected to pose a serious impact on the agricultural systems and crop productivity. These will likely put the local communities at a higher risk. The scale of the impact could be large due to the size of the affected population (see Fig. 1), the vulnerability of the poor farmers, and the lack of adaptive institutional capacity to manage the impacts (UNEP, 2009).

Water-related aspects of climate, such as droughts and floods have serious implications for African countries' development. Drought has been one of the most frequent climate-related phenomena occurring across large portions of the African continent, often with devastating consequences for the agricultural production and food security (Rojas et al., 2011). As projected in this study, northern regions of the continent will experience more severe droughts. Some eastern and southern regions of the continent will also experience lesser rainfalls (Fig. 6), smaller blue water and green water availability (Figs. 8 and 10, respectively), and longer periods without a major rainfall event (Fig. 14) combined with larger annual variations. Hence they are susceptible to more severe drought conditions. In the countries of southern and eastern Africa situated in semi-arid regions, the rain-fed agricultural production is mainly limited by the availability of soil moisture. Heavy rains often do not significantly increase soil moisture, but tend to produce runoff without infiltrating into the soil. The problems are aggravated by the tendency of prolonged dry periods to occur at irregular intervals under the future climate change.

The general trend of decreasing runoff (blue water resources) could increase conflicts over water in the shared rivers. In Africa, river channels and basin watersheds frequently demarcate international boundaries, making up almost 40% of these borders. All major African rivers traverse international boundaries. (De Wit and Stankiewicz, 2006). To what extent the reduced flow in major rivers reflects direct changes in rainfall, runoff, discharge and groundwater flow requires further study.

4.3. Study limitations

It must be pointed out that the predictions of hydrological components in the current study were based on the use of the same land cover for the historic as well as the future period. This may have under estimated the AET, as denser vegetation and larger AET are expected to increase with higher temperature and CO₂ concentration in the future (Abbaspour et al., 2009). In addition, the study does not consider any changes in the soil parameters in the future. Land use changes such as urbanization, re- and deforestation change surface properties, which in turn affect partitioning of rainfall into runoff and infiltration. Also, soil erosion that is widespread in Africa, changes soil properties and may lead to a different response of soil in partitioning the infiltrated water between AET, soil moisture, and deep aquifer recharge (Setegn et al., 2011). Therefore, an advanced study of climate change impact assessment while considering the land cover and soil

parameter changes would increase the confidence on the projected results.

Another area of concern that warrants more research is the use of data set embedding five GCMs in this study. Although scenarios and GCMs designed to cover 93% of future uncertainty in 21st century (Mitchell et al., 2004), perusing a thorough investigation based on combined effect of other GCMs or RCMs might result different outcomes.

Acknowledgements

The authors thank Eawag, Swiss Federal Institute of Aquatic Science and Technology for supporting this publication. We are especially indebted to the anonymous reviewers for valuable comments on an earlier version of the manuscript.

References

- Abbaspour, K.C., 2011. User Manual for SWAT-CUP: SWAT Calibration and Uncertainty Analysis Programs. Eawag: Swiss Fed. Inst. of Aquat. Sci. and Technol., Duebendorf, Switzerland, 103 pp. <http://www.eawag.ch/organization/abteilungen/siam/software/swat/index_EN>.
- Abbaspour, K.C., Faramarzi, M., Ghasemi, S., Yang, H., 2009. Assessing the impact of climate change on water resources in Iran. *Water Resour. Res.* 45, W10434.
- Agoumi, A., 2003. Vulnerability of North African Countries to Climatic Changes: Adaptation and Implementation Strategies for Climatic Change. IISD, 14 pp. <http://www.cckn.net/pdf/north_africa.pdf>.
- Andersson, L., Samuelsson, P., Kjellstrom, E., 2011. Assessment of climate change impact on water resources in the Pungwe river basin. *TELLUS Ser. A – Dyn. Meteorol. Oceanogr.* 63, 138–157.
- Arnell, N.W., Livermore, M.J.L., Kovats, S., Levy, P.E., Nicholls, R., Parry, M.L., Gaffin, S.R., 2004. Climate and socio-economic scenarios for global-scale climate change impacts assessments: characterising the SRES storylines. *Global Environ. Change* 14, 3–20.
- Arnold, J.G., Srinivasan, R., Muttiah, R.S., Williams, J.R., 1998. Large area hydrologic modeling and assessment – Part 1: model development. *J. Am. Water Resour. Assess.* 34, 73–89.
- Beyene, T., Lettenmaier, D.P., Kabat, P., 2010. Hydrologic impact of climate change on the Nile river basin: implications of the 2007 IPCC scenarios. *Clim. Change* 100, 433–461.
- Boko, M., Niang, I., Nyong, A., Vogel, C., Githeko, A., Medany, M., Osman-Elasha, B., Tabo, R., Yanda, P., 2007. Africa. In: Parry, M.L., Canziani, O.F., Palutikof, J.P., van der Linden, P.J., Hanson, C.E. (Eds.), Contribution of working group II to the fourth assessment report of the intergovernmental panel on climate change. Cambridge University Press, Cambridge, 433–467.
- CEEPA, 2006. District Level Hydroclimatic Time Series and Scenario Analysis to Assess the Impacts of Climate Change on Regional Water Resources and Agriculture in Africa. Discussion Paper No. 13. Special Series on Climate Change and Agriculture in Africa, 60 pp. ISBN 1-920160-01-09.
- Cox, P., Stephenson, D., 2007. A changing climate for prediction. *Science* 317, 207–208.
- Dai, A.G., 2011. Drought under global warming: a review. *WILEY Interdiscipl. Rev – Clim. Change* 2 (1), 45–65. <http://dx.doi.org/10.1002/wcc.81>.
- de Wit, M., Stankiewicz, J., 2006. Changes in surface water supply across Africa with predicted climate change. *Science* 311, 1917–1921.
- Eckhardt, K., Ulbrich, U., 2003. Potential impacts of climate change on groundwater recharge and streamflow in a central European low mountain range. *J. Hydrol.* 284, 244–252.
- Falkenmark, M., Rockstrom, J., 2006. The new blue and green water paradigm: breaking new ground for water resources planning and management. *J. Water Resour. Plan. Manage.* ASCE 132, 129–132.
- Faramarzi, M., Abbaspour, K.C., Schulin, R., Yang, H., 2009. Modelling blue and green water resources availability in Iran. *Hydrol. Process.* 23, 486–501.
- Fontaine, T.A., Klassen, J.F., Cruickshank, T.S., Hotchkiss, R.H., 2001. Hydrological response to climate change in the Black Hills of South Dakota, USA. *Hydrol. Sci. J.* 46, 27–40.
- Food and Agriculture Organization (FAO), 2006. The State of Food Insecurity in the World. Eradicating World Hunger-taking Stock Ten Years After the World Food Summit, Rome, Italy, 7 pp.
- Food and Agriculture Organization (FAO), 1995. The Digital Soil Map of the World and Derived Soil Properties. Version 3.5 (CD-ROM), Rome.
- Gaiser, T., Judex, M., Igue, A.M., Paeth, H., Hiepe, C., 2011. Future productivity of fallow systems in sub-Saharan Africa: is the effect of demographic pressure and fallow reduction more significant than climate change? *Agric. For. Meteorol.* 151, 1120–1130.
- Gassman, P.W., Reyes, M.R., Green, C.H., Arnold, J.G., 2007. The soil and water assessment tool: historical development, applications, and future research directions. *Trans. ASABE* 50, 1211–1250.
- Hargreaves, G., Samani, Z.A., 1985. Reference crop evapotranspiration from temperature. *Appl. Eng. Agric.* 1, 96–99.

- Intergovernmental Panel on Climate Change (IPCC), 2001. *Climate Change 2001: The Scientific Basis*. Cambridge Univ. Press, Cambridge, UK.
- Intergovernmental Panel on Climate Change (IPCC), 2007. *Climate Change 2007: Impacts, Adaptation, and Vulnerability, Contribution of Working Group II to the Third Assessment Report of the Intergovernmental Panel on Climate Change*. In: Parry, M.L. et al. (Eds.). Cambridge Univ. Press, Cambridge, UK.
- Jinming, F., Congbin, F., 2006. Inter-comparison of 10-year precipitation simulated by several RCMs for Asia. *Adv. Atmos. Sci.* 23, 531–542.
- Kahinda, J.M., Taigbenu, A.E., Boroto, R.J., 2010. Domestic rainwater harvesting as an adaptation measure to climate change in South Africa. *Phys. Chem. Earth* 35, 742–751.
- Krause, P., Boyle, D.P., Base, F., 2005. Comparison of different efficiency criteria for hydrological model assessment. *Adv. Geosci.* 5, 89–97.
- Krysanova, V., Dicksen, C., Timmerman, J., Varela-Ortega, C., Schluter, M., Roest, K., Huntjens, P., Jaspers, F., Buiteveld, H., Moreno, E., Carrea, J.P., Slamova, R., Marinkova, M., Blanco, I., Esteve, P., Pringle, K., Pahl-Wostl, C., Kabat, P., 2010. Cross-comparison of climate change adaptation strategies across large river basins in Europe, Africa, and Asia. *Agric. Water Manage.* 24, 4121–4160.
- Kysely, J., Beranova, R., 2009. Climate-change effects on extreme precipitation in central Europe: uncertainties of scenarios based on regional climate models. *Theor. Appl. Climatol.* 95, 361–374.
- Liu, J., Fritz, S., van Wesenbeeck, C.F.A., Fuchs, M., You, L., Obersteiner, M., Yang, H., 2008. A spatially explicit assessment of current and future hotspots of hunger in sub-Saharan Africa in the context of global change. *Global Planet. Change* 64, 222–235.
- Maurer, E.P., Adam, J.C., Wood, A.W., 2009. Climate model based consensus on hydrologic impacts of climate change to Rio Lempa basin of central America. *Hydrol. Earth Syst. Sci.* 13, 183–194.
- Milly, P.C.D., Dunne, K.A., Vecchia, A.V., 2005. Global pattern of trends in streamflow and water availability in a changing climate. *Nature* 438 (17), 347–350.
- Mitchell, T.D., Carter, T.R., Jones, P.D., Hulme, M., New, M., 2004. A Comprehensive Set of High-resolution Grids of Monthly Climate for Europe and the Globe: The Observed Record (1901–2000) and 16 Scenarios (2001–2100). Working Paper 55, Tyndall Centre for Climate Change Research, University of East Anglia, Norwich.
- Mitchell, T.D., Jones, P.D., 2005. An improved method of constructing a database of monthly climate observations and associated high-resolution grids. *Int. J. Climatol.* 25, 693–712.
- Murray, S.J., Foster, P.N., Prentice, I.C., 2012. Future global water resources with respect to climate change and water withdrawals as estimated by a dynamic global vegetation model. *J. Hydrol.* 448, 14–29.
- Neitsch, S.L., Arnold, J.G., Kiniry, J.R., Williams, J.R., 2005. Soil and Water Assessment Tool. Theoretical Documentation: Version 2000. TWRTR-191. Texas Water Resources Institute, College Station, TX.
- NEPAD. 2001. *The New Partnership for Africa's Development*. Abuja, Nigeria, 59 pp.
- New, M., Hulme, M., Jones, P.D., 2000. Representing twentieth century space-time climate variability. Part 2: development of 1901–96 monthly grids of terrestrial surface climate. *J. Clim.* 13, 2217–2238.
- Odney, D.A., 2007. The potential of pigeon pea (*Cajanus cajan* (L.) Millsp.) in Africa. *Nat. Resour. Forum* 31, 297–305.
- Orlowsky, B., Seneviratne, S.I., 2012. Global changes in extreme events: regional and seasonal dimension. *Clim. Change* 110, 669–696.
- Ritchie, J.T., 1972. A model for predicting evaporation from a row crop with incomplete cover. *Water Resour. Res.* 8, 1204–1213.
- Rojas, O., Vrieling, A., Rembold, F., 2011. Assessing drought probability for agricultural areas in Africa coarse resolution remote sensing imagery. *Remote Sens. Environ.* 115, 343–352.
- Rowhani, P., Lobell, D.B., Linderman, M., Ramankutty, N., 2011. Climate variability and crop production in Tanzania. *Agric. For. Meteorol.* 151 (4), 449–460.
- Ruelland, D., Ardoin-Bardin, S., Collet, L., Roucou, P., 2012. Simulating future trends in hydrological regime of a large Sudano-Sahelian catchment under climate change. *J. Hydrol.* 424, 207–216.
- Schlenker, W., Lobell, D.B., 2010. Robust negative impacts of climate change on African agriculture. *Environ. Res. Lett.* 5, 014010.
- School, J., Abbaspour, K.C., Srinivasan, R., Yang, H., 2008. Modelling blue and green water availability in Africa. *Water Resour. Res.* 44, W07406.
- School, J., Abbaspour, K.C., 2007. A daily weather generator for predicting rainfall and maximum–minimum temperature using monthly statistics based on a half-degree climate grid. *Ecol. Model.* 201, 301–311.
- Semenov, M.A., Stratonovitch, P., 2010. Use of multi-model ensembles from global climate models for assessment of climate change impacts. *Clim. Res.* 41, 1–14.
- Setegn, S.G., Rayner, D., Melesse, A.M., Dargahi, B., Srinivasan, R., 2011. Impact of climate change on the hydroclimatology of Lake Tana basin, Ethiopia. *Water Resour. Res.* 47, W04511.
- Shongwe, M.E., van Oldenborgh, G.J., van den Hurk, B.J.J.M., de Boer, B., Coelho, C.A.S., van Aalst, M.K., 2009. Projected changes in mean and extreme precipitation in Africa under global warming. Part I: southern Africa. *J. Clim.* 22, 3819–3837.
- Sowers, J., Vengosh, A., Weinthal, E., 2011. Climate change, water resources, and the politics of adaptation in the Middle East and north Africa. *Clim. Change* 104, 599–627.
- Stockle, C.O., Williams, J.R., Rosenberg, N.J., Jones, C.A., 1992. A method for estimating the direct and climatic effects of rising atmospheric carbon dioxide on growth and yield of crops: Part 1. Modification of the EPIC model for climate change analysis. *Agric. Syst.* 38, 225–238.
- Stonefelt, M.D., Fontaine, T.A., Hotchkiss, T.H., 2000. Impacts of climate change on water yield in the Upper Wind river basin. *J. Am. Water Resour. Assess.* 36, 321–336.
- Tao, F., Zhang, Z., Liu, J., Yokozawa, M., 2009. Modelling the impacts of the weather and climate variability on crop productivity over a large area: a new super-ensemble-based probabilistic projection. *Agric. For. Meteorol.* 149, 1266–1278.
- Taye, M.T., Ntegeta, V., Ogiramo, N.P., Willems, P., 2011. Assessment of climate change impact on hydrological extremes in two source regions of the Nile river basin. *Hydrol. Earth Syst. Sci.* 15, 209–222.
- Thompson, H.E., Berrang-Frd, L., Ford, J.D., 2010. Climate change and food security in sub-Saharan Africa: a systematic literature review. *Sustainability* 2, 2719–2733.
- Thornton, P., Jones, P.G., Alagarswamy, G., Andersson, J., 2009. Spatial variation of crop yield response to climate change in east Africa. *Global Environ. Change* 19, 54–65.
- UN Millennium Project, 2005. *Halving Hunger: It can be Done*. Earthscan, London, 242 pp.
- UNEP, 2009. *Assessment of Transboundary Freshwater Vulnerability to Climate Change*. <http://www.unep.org/dewa/Portals/67/pdf/Assessment_of_Transboundary_Freshwater_Vulnerability_revised.pdf>.
- UNESCO, 1979. *Map of the World Distribution of Arid Regions: Explanatory Note*. MAP Technical Notes 7. UNESCO, Paris, 54 pp.
- Vörösmarty, C.J., Douglas, E.M., Green, P.A., Revenga, C., 2005. Geospatial indicators of emerging water stress: an application to Africa. *Ambio* 34 (3), 230–236.
- Vörösmarty, C.J., McIntyre, P.B., Gessner, M.O., Dudgeon, D., Prusevich, A., Green, P., Glidden, S., Bunn, S.E., Sullivan, C.A., Reidy Liermann, C., Davies, P.M., 2010. Global threats to human water security and river biodiversity. *Nature* 467, 555–561.
- Williams, J.R., Jones, C.A., Dyke, P.T., 1984. A modeling approach to determining the relationship between erosion and soil productivity. *Trans. ASAE* 27 (1), 129–144.
- World Bank, 1995. *From Scarcity to Security: Averting a Water Crisis in the Middle East and North Africa*. Washington, DC. GTZ 1998.
- You, L., Ringler, C., Nelson, G., Wood-Sichra, U., Roberston, R., Wood, S., Guo, Z., Zhu, T., Sun, Y., 2010. What is the Irrigation Potential for Africa? A Combined Biophysical and Socioeconomic Approach. Environment and Production Technology Division. IFPRI Discussion Paper 00993, 30 pp.
- Ziervogel, G., Bharwani, S., Downing, T.E., 2006. Adapting to climate variability: pumpkins, people and policy. *Nat. Resour. Forum* 30, 294–305.
- Ziervogel, G., Johnston, P., Matthew, M., Mukheibir, P., 2010. Using climate information for supporting climate change adaptation in water resource management in South Africa. *Clim. Change* 103, 537–554.